Desalination and Water Treatment
www.deswater.com
20 (2010) 11–21
August
1944-3994 / 1944-3986 © 2010 Desalination Publications. All rights reserved.
doi: 10.5004/dwt.2010.1207

Numerical simulation and experimental validation of a controlled flow solar water disinfection system

H.H. El Ghetany[a], A. Abdel Dayem[b]*

[a]*National Research Centre, Solar Energy Department, El-Tahrir St., Dokki, Cairo, Egypt, email: helghetany@hotmail.com*
[b]*Mechanical Power Engineering Department, Faculty of Engineering, Mattarria, Helwan University, 11718 Cairo, Egypt email: adel_abdeldayem@hotmail.com*

Received 12 May 2009; Accepted in revised form 9 February 2010

ABSTRACT

A controlled flow solar thermal disinfection system was manufactured, tested and numerically investigated. The system is simply constructed of a 2.34 m² flat-plate solar collector at which the outlet flow temperature is controlled by a solenoid valve to a disinfection temperature. The outlet hot disinfected water is used to preheat the inlet untreated water through a heat exchanger. Different disinfection temperatures are considered with their corresponding heating periods of time. The system is numerically simulated to investigate their annual performance and life cycle savings. The simulation model is validated by measured data with close agreement. It is obtained that the considered simple system working at 60°C disinfection temperature can daily produce 171 l of clean water by m² of solar collector where it reduces into about 39 l/m² at 90°C. That corresponds to 81.5 and 1.1 l/m² per kWh of incident solar radiation respectively. The disinfected liter of water can cost about US$ 0.00001 along the system lifetime.

Keywords: Collector controlled flow; Solar heating; Numerical simulation; Water disinfection

1. Introduction

In thermal disinfection, water is simply heated to a preset temperature for a specified heating time. The time is taken longer for low temperatures than in high ones. Therefore this research aims to study the performance of a controlled flow solar water system for thermally disinfected water for temperatures up to 100°C. At these temperatures, water and other liquids can be pasteurized because most of enteric viruses, bacteria and parasites are rapidly inactivated [1]. The water temperature that reaches 65°C, called a pasteurization temperature, is capable of inactivating nearly all enteric pathogens within several tens of minutes to hours [2]. The flat-plate collectors can be simply and efficiently utilized in that temperature levels using low cost components. The pasteurization period of time can be adjusted by a solenoid valve. Moreover, the outlet hot disinfected water can be reused to preheat the inlet untreated cold water to the collector. In that case, the collector can raise the water into few degrees of temperature with a large flow rate production.

Regarding the edited work in this area, Bansal et al. [3] presented the principles of the thermosiphone solar water heating to create an overflow area in flat plate solar collectors that can be used for sterilization of water. They found that a single flat plate solar collector was able to produce hot water at 80°C on hourly basis of average of

* Corresponding author. Current address: Umm Al-Qura University, College of Engineering, Mechanical Engineering Department, Makkah, P.O. 05555, KSA, Tel. +966 (2) 5270000; Fax +966 (2) 5270027; email: amabdeen@uqu.edu.sa

3.6 l/m² for each kWh of incident solar energy. El-Ghetany and El-Seesy [4] studied the performance evaluation of overflow thermosiphonic solar water heating at different thermosiphonic heads. They concluded that the flat plate collector was able to produce hot water at 70°C on hourly basis of average of 2.85 l/m² for each kWh of incident solar energy. While El-Seesy [5] conducted to study the performance of the flat plate solar collector and concluded that the solar flat plate collector can produce hot water at 70°C on hourly basis of average of 3.18 l/m² for each kWh of incident solar energy. David et al. [6] constructed a solar hot box cooker for pasteurizing purposes. It ensures that the water will be above the milk pasteurization temperature of 62.8°C for at least 1 h, which appears sufficient to pasteurize untreated water. The same conclusions can be found by Schitzer et al. [7] and Morrison and Braun [8].

Oates et al. [9] developed a mathematical model to show the inactivation of total coliform, *E. coli*, and H_2S-producing bacteria in water by direct incident solar radiation. They found that one-day exposure achieved complete bacterial inactivation 52% of the time, while a 2-day exposure period achieved complete microbial inactivation 100% of the time.

McLoughlin et al. [10] compared three different collectors of compound parabolic, parabolic and V-groove profiles for the disinfection of water heavily contaminated with *Escherichia coli* (K-12). Results have shown that the compound parabolic reflector promoted a more successful inactivation of *E. coli* than the parabolic and V-groove profiles. In addition, Fernández et al. [11] reviewed the viability of solar photocatalysis for disinfection in low cost compound parabolic collectors, using sunlight and titanium dioxide (TiO_2) semiconductor, both applied as slurry and supported.

Martin-Dominguez [12] presented the efficiency of the solar exposure based water disinfection process inside colored bottles. With the use of solar concentrators and partially blackened bottles, the water temperature reached 65°C, while only 50°C was achieved when using the same concentrators and completely transparent bottles.

Duff and Hodgson [13] designed, built and tested a new passive solar water pasteurization system based on density difference flow principles. The system with a total absorber area of 0.45 m² has achieved a peak flow rate of 19.3 kg/h of treated water. Moreover the paper of Scrivani et al. [14] examines the concept of utilizing trough type solar concentration plants for water production, remediation and waste treatment. They discussed their potential economical and environmental benefits of using solar trough collectors in water treatment.

Rincón and Pulgarin [15] carried out experiments using a compound parabolic concentrating collector (CPC) and natural water spiked with *E. coli* K 12. The addition of TiO_2, TiO_2/Fe^{3+} or Fe^{3+}/H_2O_2 to the water accelerates the bactericidal action of sunlight, leading to total disinfection by solar photocatalysis. Further, Navntoft et al. [16] tested CPC collector to enhance solar disinfection with natural well-water and natural sunlight conditions.

The objectives of the present study can be summarized in the following points. (a) to experimentally verify the presented study of a controlled flow solar disinfection water heating system under the environmental conditions of Cairo, Egypt, (b) to build up a validated mathematical model for the controlled-flow solar-water-heating-system to investigate the annual performance of the system. (c) to evaluate the outlet hot water per solar radiation dose (kWh/m²) at different outlet temperatures.

2. Experimental setup

In the published work the solar water disinfection was carried out by either optical or thermal methods. In thermal methods, thermosyphone flat-plate collectors and concentrating collectors were used. In the present system a flat-plate collector with controlled self-preheated flow was efficiently used to maximize the productivity. The considered solar water disinfecting system consisted of six components:

- flat-plate solar collector
- untreated water tank
- clean water tank
- shell and tube heat exchanger
- control device unit (solenoid valve)

Solar water flat-plate collector is a device in which water is heated by solar energy absorbed. It is simple to manufacture and it is relatively cost effective. The absorber was fabricated from 11 steel fins 160 cm × 11 cm and 0.05 cm thickness. 9 copper tubes, 7 mm diameter, were lined with them. The absorber was painted with black matt paint to increase its absorptivity. The distance between the glass cover and absorber plate was 5 cm. The heat loss by conduction was reduced by insulating the bottom and sides of the casing with glass wool of 5 cm thickness. The absorber and insulation were then installed in wood casing of 2 cm thickness. Its dimensions were 194 cm × 124 cm × 10 cm. The casing was covered with a single window glass of 4 mm thickness to reduce the convection heat losses. Rubber gasket 2 cm wide was sealed on the inner edges of the casing under the glass to prevent leakage of the air. The collector was tested using a local standard collector test rig at G_{test} of 171 kg/m² and about 800 W/m² solar radiation. It was found that the collector efficiency curve has $F_R\ \tau\alpha = 0.3361$ and $F_R\ U_L = 1.4266$ W/m².C.

A shell and tube heat exchanger was designed and fabricated to be installed through the system. The total surface area was 0.016 m² with one shell and twenty tubes; 12.5 mm diameter cooper tubes. The external casing was made from 1 mm galvanized steel sheet and insulated by 5-cm thick glass wool insulation from all sides.

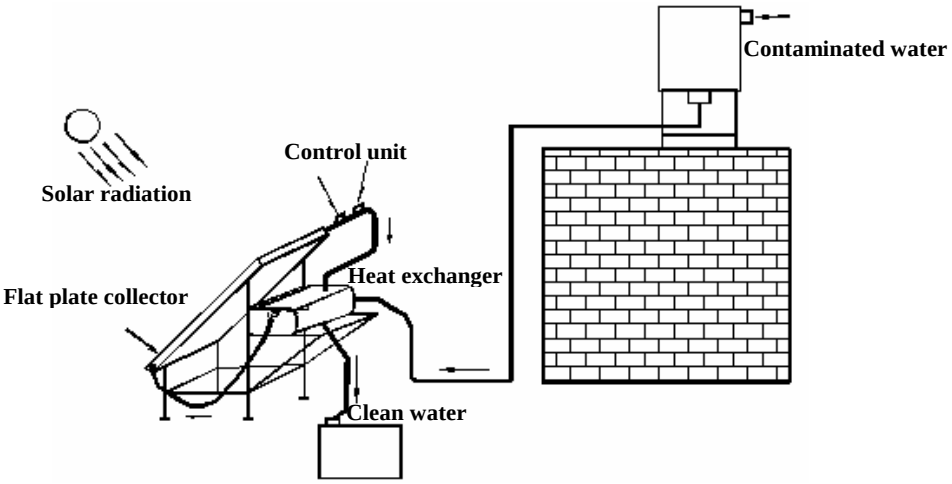

Fig. 1. Schematic diagram of the solar water disinfecting system installation.

The untreated water passed through the collector under 4 m head pressure from a 200 l untreated tank located 4 m above the collector plan as shown in Fig. 1. By that water flowed by only gravity therefore it could develop a uniform flow inside the collector and control the water flow rate of the collector. The setup was provided with necessary measuring instruments to carry out the required tests.

The measuring instruments used in the experimental tests were implemented to measure the tested parameters to evaluate the thermal performance of the controlled flow solar water heating system at different operating conditions. A thermopile pyranometer of Kipp & Zonen type (model CM5-774035) was used to measure the instantaneous data of the total solar radiation intensity (IT) incident on the collector surface. It was connected to a multi range single function meter of Kaise type (model SK-5000K). The output voltage of the pyranometer was 6.09×10^{-3} mV/Wm^{-2} for a resistance range of 10 Ohm.

In order to utilize the solar collector as a heating source to produce water at fixed temperature, to be used in disinfecting techniques, a control device was placed at the collector exit. It consisted of a solenoid valve (normally closed) and a thermostat. The thermostat was an electronic temperature controller of JTC-903 type and the temperature range of 0–400°C working with 220 V and 50 Hz frequency. As an example, if the desired temperature used for water disinfection was (70°C), so the thermostat was adjusted to the desired temperature. The solenoid valve did not allow the water to flow until an electric signal was received from the thermostat informing that the water temperature reached the desired value. When the solenoid valve was opened, the disinfected hot water was passed through the heat exchanger to heat the incoming untreated water prior entering the solar collector to reduce the heating time.

Ten k-type thermocouples were placed in different locations of the system to measure inlet and outlet water temperature of the collector, absorber plate temperature distribution and glass temperatures as shown in Fig. 2. They were equally distributed along the vertical side of the collector with about 28 cm apart. Two points were measured on the glass surface where they divided it into equal three parts. The thermocouples were connected to the digital dual input thermometer (type K). It was of BK Precision type (model 710). A volume scale was used to measure the quantity of disinfecting water with 20 ml accuracy.

3. Mathematical model

The performance of a system component will normally depend upon characteristic fixed parameters. The performance (or outputs) of other components, and time-dependent forcing functions for a solar water disinfecting

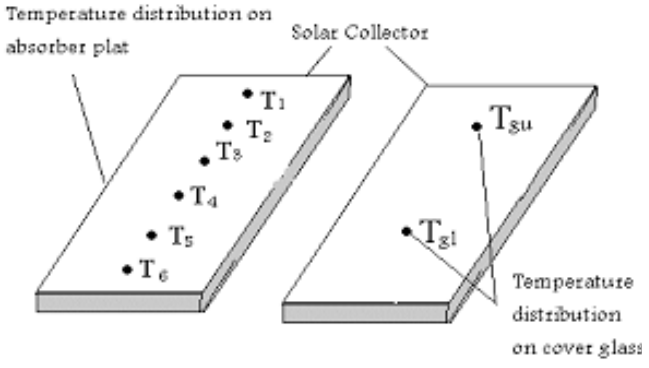

Fig. 2. Locations of temperature measurements equally distributed along the collector absorber and the glass cover.

system, knowledge of the weather (i.e., solar radiation, ambient temperature etc.) and the hot water demand as a function of time are necessary in order to determine the transient system performance. Because the system consists of components, it is necessary to simulate the performance of the system by collectively simulating the performance of the interconnected components.

As explained in the experimental work, the considered system was simply constructed. It contained a flat-plate collector connected with a solenoid valve. A shell and tube heat exchanger was conducted to reuse the hot water produced as a pre-heater. The solenoid valve was replaced by a pump switched by an on/off control unit in the simulation modeling. The control unit switched the outlet collector temperature to the predefined value. Accordingly, the simulated system consisted of a switched pump with 450 l/h (such that is used in the experimental setup) flow rate pumping cold water into the cold side of a shell/tube heat exchanger. Where the outlet cold flow of the heat exchanger went to the collector, the collector outlet was the input of the heat exchanger hot side. The following subsections indicate the governing equations of each system component used to simulate their performance.

3.1. Flat-plate collector

The constructed collector was a flat-plate collector with 2.34 m² oriented to the south and sloped 30° with the horizontal (equal the latitude angle of Cairo). A general expression for collector efficiency can be obtained from the Hottel–Whillier equation as [17]

$$\eta = \frac{Q_u}{A_c I_T} = F_R \tau\alpha - F_R U_L \frac{(T_i - T_a)}{I_T} \tag{1}$$

In order to account for conditions when the collector was operated at a flow rate other than the value at which it was tested, both $F_R(\tau\alpha)$ and $F_R U_L$ were corrected to account for changes in F_R. The ratio, r_1, by which they were corrected, is given by [17]:

$$r_1 = \frac{\dfrac{\dot{m}_c C_p}{A_c F U_L}\left(1 - e^{-A_c F U_L / \dot{m} C_p}\right)\Big|_{use}}{\dfrac{\dot{G}_{test} C_p}{F U_L}\left(1 - e^{-F U_L / G_{test} C_p}\right)} \tag{2}$$

The parameter $F'U_L$ was considered to be independent of flow rate and was calculated using the test flow rate as [17]

$$F'U_L = -G_{test}.C_{Pc} \ln\left(1 - \frac{F_R U_L}{G_{test}.C_{Pc}}\right) \tag{3}$$

The intercept efficiency, $F_R(\tau\alpha)_n$, was corrected for non-normal solar incidence by the factor $(\tau\alpha)/(\tau\alpha)_n$. By definition, $(\tau\alpha)$ is the ratio of the total absorbed radiation to the incident radiation. Thus, a general expression for $(\tau\alpha)/(\tau\alpha)_n$ is [17]

$$\frac{(\tau\alpha)}{(\tau\alpha)_n} = \frac{I_{bT}\dfrac{(\tau\alpha)_b}{(\tau\alpha)_n} + I_d\left(\dfrac{1+\cos\beta}{2}\right)\dfrac{(\tau\alpha)_s}{(\tau\alpha)_n} + \rho_g I\left(\dfrac{1-\cos\beta}{2}\right)\dfrac{(\tau\alpha)_g}{(\tau\alpha)_n}}{I_T} \tag{4}$$

For flat-plate collectors, $(\tau\alpha)_b/(\tau\alpha)_n$ can be approximated from ASHRAE test results [18] as

$$\frac{(\tau\alpha)_b}{(\tau\alpha)_n} = 1 - b_0\left(\frac{1}{\cos\theta} - 1\right) - b_1\left(\frac{1}{\cos\theta} - 1\right)^2 \tag{5}$$

3.2. Pump

This pump model computed a mass flow rate using a variable control function, which must be between zero and one, and a fixed (user specified) maximum flow capacity. Pump power consumption may also be calculated as a linear function of mass flow rate.

$$T_o = T_i + \frac{P \cdot f_{par}}{m C_p} \tag{6}$$

3.3. Shell and tube heat exchanger

A zero capacitance sensible heat exchanger was modeled in the shell and tube mode. For given hot and cold side inlet temperatures and flow rates, the effectiveness was calculated for a given fixed value of the overall heat transfer coefficient. The mathematical description that follows was covered in details in DeWitt and Incropera [19].

$$C_c = m_c C_{pc} \tag{7}$$

$$C_h = m_h C_{ph} \tag{8}$$

C_{max} = maximum value of C_h and C_c

C_{min} = minimum value of C_h and C_c

$$\varepsilon_1 = 2\left\{1 + \frac{C_{min}}{C_{max}} + \left(1 + \left(\frac{C_{min}}{C_{max}}\right)^2\right)^{0.5} \times \frac{1 + \exp\left[-\dfrac{UA}{C_{min}}\left(1 + \left(\dfrac{C_{min}}{C_{max}}\right)^2\right)^{0.5}\right]}{1 - \exp\left[-\dfrac{UA}{C_{min}}\left(1 + \left(\dfrac{C_{min}}{C_{max}}\right)^2\right)^{0.5}\right]}\right\}^{-1} \tag{9}$$

$$\varepsilon = \left[\left(\frac{1-\varepsilon_1\frac{C_{\min}}{C_{\max}}}{1-\varepsilon_1}\right)^N - 1\right]\left[\left(\frac{1-\varepsilon_1\frac{C_{\min}}{C_{\max}}}{1-\varepsilon_1}\right)^N - \frac{C_{\min}}{C_{\max}}\right]^{-1} \quad (10)$$

$$T_{ho} = T_{hi} - \varepsilon\left(\frac{C_{\min}}{C_h}\right)\left(T_{hi} - T_{ci}\right) \quad (11)$$

$$Q_T = \varepsilon C_{\min}\left(T_{hi} - T_{ci}\right) \quad (12)$$

If $C_{min}/C_{max} \le 0.01$, then

$$\varepsilon = 1.0 - \exp\left(\frac{UA}{C_{\min}}\right) \quad (13)$$

3.4. Control unit

This controller generated a control function γ_o that can have values of 0 or 1. The value of γo was chosen as a function of the difference between upper and lower temperatures, T_H and T_L, compared with two dead band temperature differences, ΔT_H and ΔT_L. The new value of γ_o is dependent on whether the initial value γ_i = 0 or 1. The controller was normally used with γ_o connected to γ_i giving a hysteretic effect.

3.5. Economic analysis

This component performed a standard life cycle cost analysis based on the simulation of one year of solar system operation. It compared the capital and back-up fuel costs of a solar system to the fuel costs of a conventional non-solar system. It was assumed that the solar back-up system is identical to the conventional heating system, in that only the incremental costs of adding solar to the conventional system are considered. The life cycle savings were calculated using P_1 and P_2 as defined by Brandemuehl and Beckman [20].

$$\mathrm{LCS} = P_1\left[\int_0^t C_{FL}\dot{Q}_{\mathrm{load}}dt - \int_0^t \dot{C}_{FA}\dot{Q}_{\mathrm{aux}}dt\right] + P_2\left[C_A \cdot A + C_E\right] \quad (14)$$

$$P_1 = \left(1 - C\bar{t}\right)\cdot PWF\left(NE, iFCF, d\right)$$
$$P_2 = D + (1-D)\frac{PWF\left(N_{\min}, 0, d\right)}{PWF\left(N_L, 0, m\right)} \quad (15)$$

$$-(1-d)\bar{t}\left[PWF\left(N_{\min}, m, d\right)\left(m - \frac{1}{PWF\left(N_L, 0, m\right)}\right) + \frac{PWF\left(N_{\min}, o, d\right)}{PWF\left(N_L, 0, m\right)}\right] + \left(1 - C\bar{t}\right)M_S \cdot PWF\left(N_E, i_g, d\right) \quad (16)$$

$$+t\left(1-\bar{t}\right)V\cdot PWF\left(N_E, i_g, d\right) - \frac{C\bar{t}}{N_D}PWF\left(N'_{\min}, 0, d\right) - \frac{SAL}{(1+d)N_E}$$

where

$\int_0^t C_{FA}Q_{\mathrm{AUX}}dt$ = total auxiliary fuel cost for the first year,

$\int_0^t \dot{C}_{FL}\dot{Q}_{\mathrm{load}}dt$ = total fuel cost of the conventional system for the first year.

The above governing equations were solved dependently together using the TRNSYS 14 simulation program [21]. The modified Euler method was used to solve the equations using a pre-defined time step 0f 0.25 h and the convergence accuracy was checked in each time step to limit the number of iterations into 30.

4. Results and discussion

The performance evaluation of the controlled flow disinfection solar water system is presented through the system temperature distributions, thermal efficiency, and the amount of hot water produced per solar radiation dose. In addition, comparing of the predicted and experimental results of the system is developed. Experiments have been carried out of the proposed system at different desired outlet water temperatures (60°C, 65°C, 70°C, 80°C and 90°C). Fig. 3 shows the instantaneous variation of the ambient temperature, and the measured global solar radiation intensity along the standard local time of the day. It is a sample of the typical weather data of clear day in Cairo, 30°N.

While Fig. 4 represents the variations of absorber plate and glass temperatures for a test run at fixed set water temperature of 90°C, the locations of the measurements

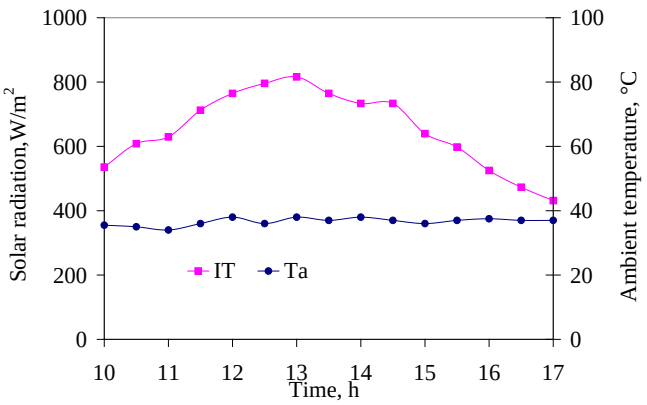

Fig. 3. Solar radiation and ambient temperature variation for a test run at fixed set water temperature of 90°C.

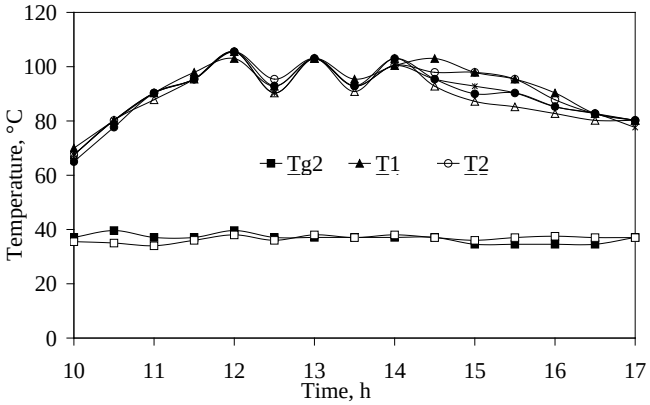

Fig. 4. Variations of absorber plate and glass cover temperatures for a test run at fixed set water temperature of 90°C.

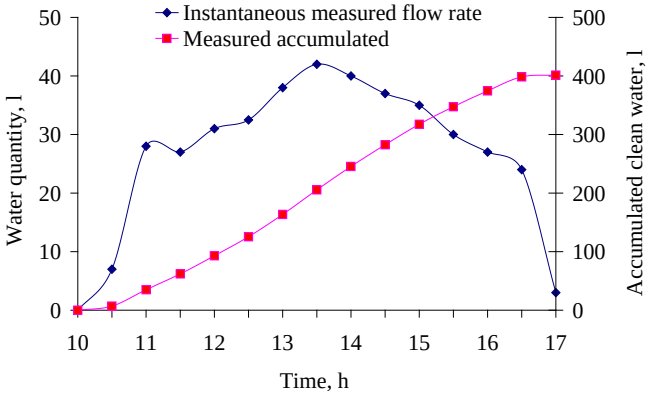

Fig. 5. The quantity and accumulated water at T_{set} = 60°C.

are indicated in Fig. 2. This experiment is developed to investigate the significance of zero flow rate on the collector temperatures. As shown in the figure, the temperature difference between the upper and lower parts of the collector absorber is about 60°C. That can be seen clearly in the upper part than in the lower part. Moreover, T6 is relatively constant along the daylight. It seems to be affected by the ambient temperature than solar radiation. It is not a big difference between it and collector inlet temperature. That can be understood in terms of the collector efficiency which is lowered due to this cause. On the other hand, the heat losses from the upper part are largely increased. That is seen clearly in the form of big difference between its temperature and glass cover temperature, it is about 35°C in average. All temperatures seem to be stagnant during the midday hours. Some changes are noticed during early and late hours due to the shading effect and the reflection of the glass cover to the inclined solar rays. The daily temperature distribution is similar to solar radiation variation. Perhaps there is a discontinuity in some times due to clouds during a day of measurements. It is an instantaneous effect.

The hot water quantity produced at different time intervals and the daily accumulated water can be presented with time at T_{set} = 60°C as shown in Fig. 5. It is found that the system is capable to produce about 400 l of hot water with T_{set} of 60°C . It is found also that the amount of hot water produced from the system at different time intervals is increased to its maximum value at noon and gradually decreased again i.e. taking the same trend of solar radiation variation.

The daily variation of the accumulated disinfected water is relatively linear due to relatively clear sky radiation during the experiments. Perhaps the solar radiation is greatly changed during the early morning and lately evening hours but that cannot produce a large amount of hot water. However for the high set temperatures the accumulated water is reduced because the collector efficiency is lowered as explained later in Figs. 11–15.

Fig. 6 presents the accumulated disinfected water l/kWh.m^2 vs. the set points of temperature. The simulation process used hourly data of the solar radiation and ambient temperature of Cairo, 30°N. It is clearly shown that the accumulated water has relatively vanished at high temperatures. The data was fitted as a non-linear function of temperature with a regression coefficient equal 0.98 and the empirical equation can be written as follows:

$$M = -0.0059\,T^3 + 1.4493\,T^2 - 119.37\,T + 3300.7 \qquad (17)$$

where M is the accumulated water in kg and T is the disinfection temperature in °C.

The numerical simulation is carried out for the considered system for one year with a quarter-hour simulation time step. The outlet temperature of the collector is switched by the control unit to 60, 65, 70, 75, 80, 85, 90 and 95°C to study the system performance under different temperature levels. The life-cycle savings of the system were determined for each temperature level.

In the simulation process, the pump is switched on until the collector outlet temperature to be lower than the set temperature (±1°C), after that the pump is switched

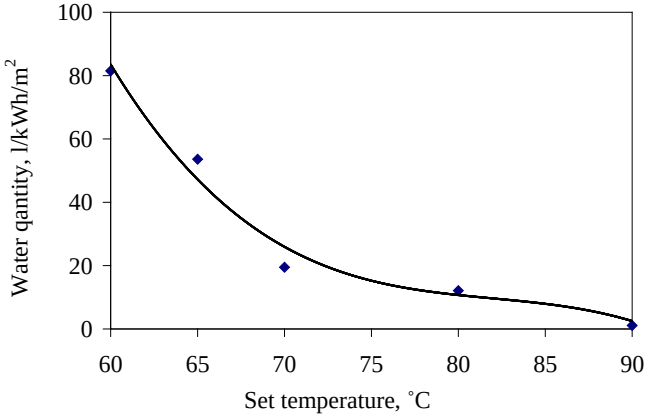

Fig. 6. The accumulated disinfected water for different temperature set points.

off. In each time step the temperatures and the flow rates can be recorded and accumulated during the system components. As a sample of the results that can be obtained, the accumulated daily quantity of disinfected water is estimated for 65°C and 90°C set temperatures. Figs. 7 and 8 show the daily water quantity along a year. Based on the weather data, the daily accumulated water is changed from day to day. Perhaps, it equals zero in some days, especially in winter days due to low solar radiation but it is largely changeable in general. The days when the daily accumulated water equals zero are the same for two set temperatures due to low solar radiation in these days. In those days the outlet temperature of the collector does not reach the predetermined set temperature. The ambient temperature has no large effect on the system performance.

In Fig. 9, the annual accumulated disinfected water and annual system efficiencies are drawn vs. the set temperatures. As expected, the water quantity is increased with lower set temperatures where the collector efficiency is decreased. This result is completely similar to the experimental one for one-day production presented in Fig. 6. The average annual efficiency of the system is defined as the accumulated hourly efficiency divided by the year hours, 8760. As shown in Fig. 9, it is decreased gradually with lower working temperatures. This is surprising but that occurred because the system is a closed system. The water is preheated in the heat exchanger before going into the collector. So, the temperature difference inside the collector is relatively small. That produces a limited quantity of useful energy.

The yearly accumulated water per kWh of solar radiation is presented vs. the set temperatures in Fig. 10. It has the same trend as in Fig. 9 where l/m² is drawn and it is similar to the experimental one indicated in Fig. 6. Certainly, each kWh can produce 32 l of disinfected water at 60°C for 1-m² collector where it can produce 0.25 l at 95°C. Accordingly, it can save 0.45 and 0.01 US$/kWh. m² respectively during the system life time as shown in Fig. 10. The life-cycle savings are estimated for each kWh of the collector outlet energy that has 1 m².

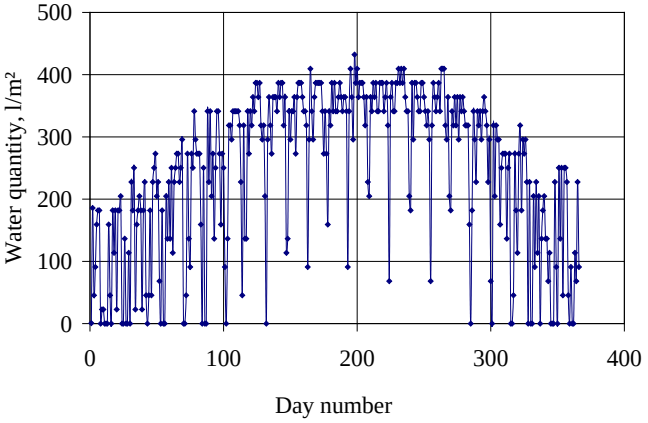

Fig. 7. Yearly daily disinfected water for set temperature of 65°C.

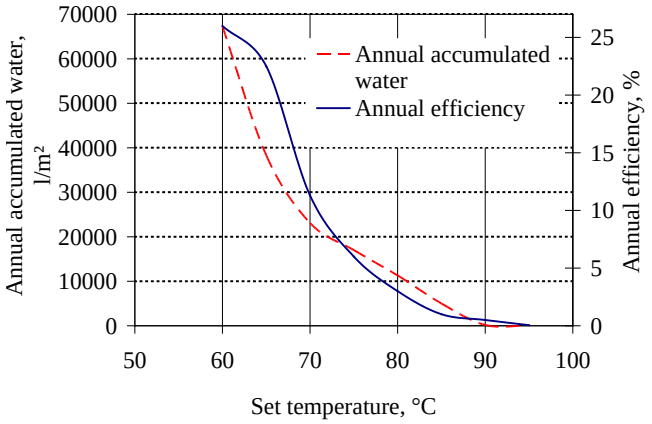

Fig. 9. Annual performance of the solar disinfection system.

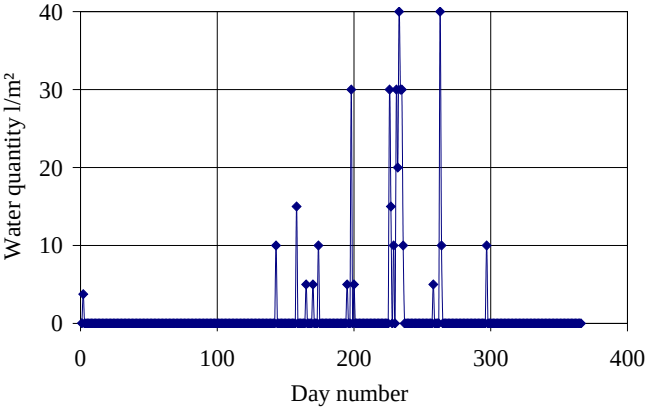

Fig. 8. Annual daily disinfected water for set temperature of 90°C.

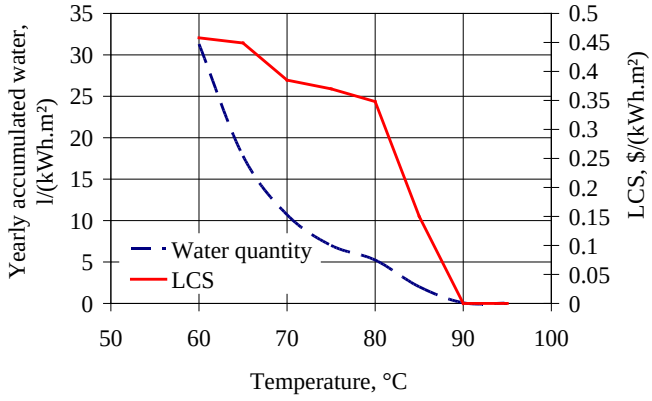

Fig. 10. Annual average disinfected water quantity and life-cycle savings vs. temperature levels.

The life cycle savings of the system are relatively low because they depend on the collector energy production in their estimation. They change linearly between the levels of temperature. The variation steeply changes about each 10°C. While they change little during low temperatures, they vary widely at the temperature more than 80°C. That is obtained due to very low efficiency of the system in condition. The collector performance is diminished with high inlet temperatures. Also they are changed slightly with changing the set temperature according to little energy output. It can be said that the system is thermally efficient using the heat exchanger as a pre-heater although the collector has a low efficiency. This fact can be found in similar heat process systems that use conventional energy sources. In such cases the heat source is used only to raise the fluid for few degrees of temperatures.

5. Comparison of numerical and experimental results

The simulation program was running for the same days in that the experiments were established using the measured solar radiation and ambient temperature for 60, 65, 70, 80 and 90°C set temperatures. The comparison between the measured and simulated data includes the time variation of the accumulated clean water. As shown in Figs. 11–15, the results for both measurements and simulation can be accepted according to the simulation capabilities. Perhaps the function of time variation for both data is not the same. In measured data, the variation seems linear especially during the midday hours for low working temperatures. For the temperature more than 70°C, the water production delayed about 2 h when the radiation was perpendicular to the collector surface. At higher temperatures water is produced around midday when the solar radiation is maximized.

The final daily accumulated water of both measurements and simulation is relatively equal, so the water quantity per kWh per 1 m^2 of the collector area is relatively the same. The water quantity is largely increased during midday when the high solar radiation is found. The difference between the measured and simulated results is due to the following reasons:

- Use of a switched pump instead of a solenoid valve that is installed in the experimental system.
- The response time of the solenoid valve and control unit.
- The collector efficiency curve was estimated locally in the lab and it seems not very fine. Accordingly, the collector performance is largely affected by its characteristics.
- In the simulation program it makes an interpolation of data for the times not have a data and that makes a difference between the actual and theoretical estimation.
- The difference between the theoretical and actual performance of the system.
- The heat capacity of the system materials that was not considered in the simulation program.
- The hold time (disinfected time) by which the water must be held inside the collector is not considered in the simulation analysis.

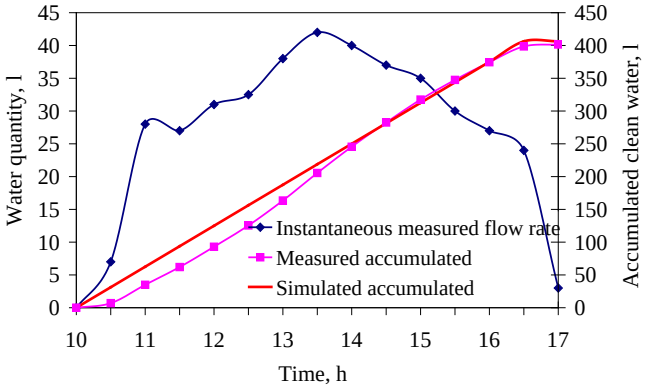

Fig. 11. Comparison between the simulated and measured accumulated clean water for the set temperature of 60°C.

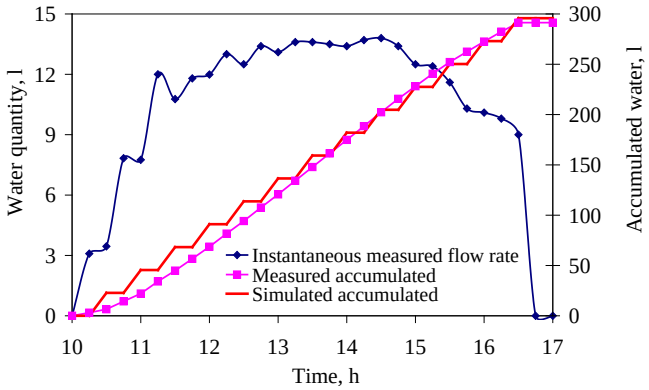

Fig. 12. Comparison between the simulated and measured accumulated clean water for the set temperature of 65°C.

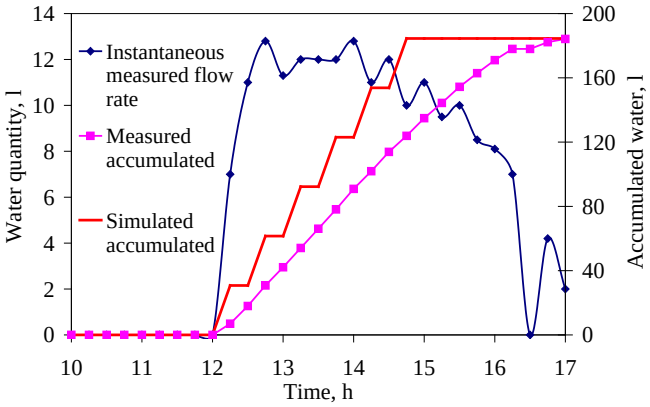

Fig. 13. Comparison between the simulated and measured accumulated clean water for the set temperature of 70°C.

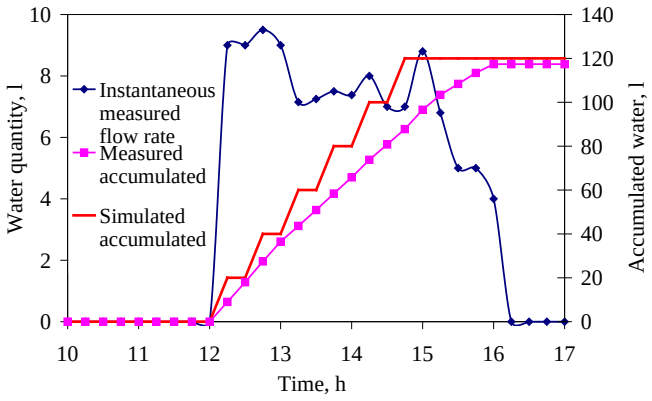

Fig. 14. Comparison between the simulated and measured accumulated clean water for the set temperature of 80°C.

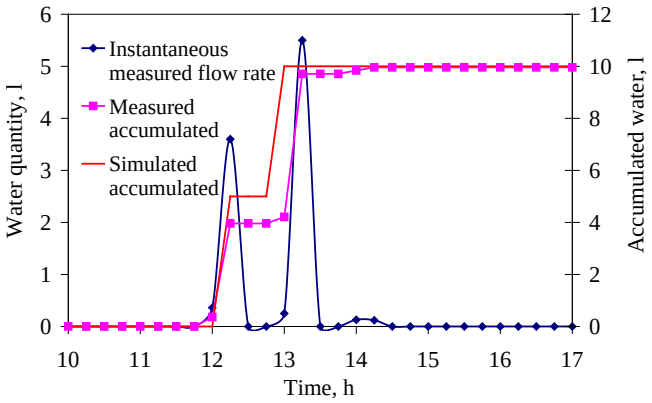

Fig. 15. Comparison between the simulated and measured accumulated clean water for the set temperature of 90°C.

The last reason has the most significance on the daily performance of the system where fifth reason affects the instantaneous performance of the system.

The experimental system performance of the present work is compared with the previous work experimentally made by El-Ghetany and El-Seesy [4] and El-Seesy [5] as shown in Fig. 16. The performance is presented by the hourly hot water quantity produced from the flat plate solar collector per solar radiation dose. As shown in Fig. 16, it is drawn vs. the collector outlet temperature. The same flat plate solar collector is used in the comparison with the same specifications. It is clear that there is a good performance agreement between the present work and the previous work especially in the higher collector outlet temperature zone while in the low temperature zone (at 60°C) there is a considerable deviation between the present work and the previous work due to the nature of utilization of each system. The controlled collector flow is used in the present system while the thermosyphonic phenomenon was considered in the other system. This deviation is developed because the collector thermosyphonic flow is low at lower temperatures. At higher

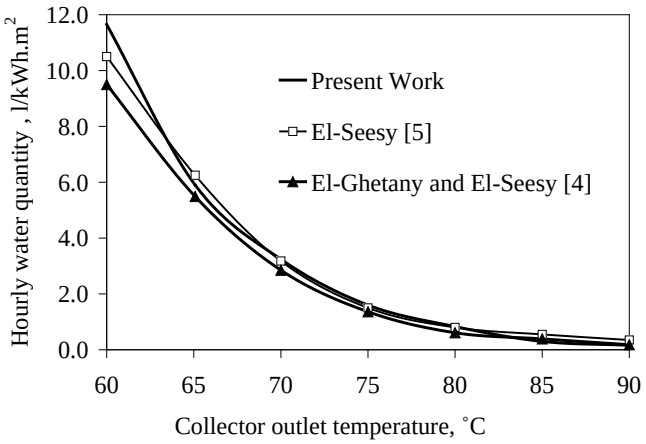

Fig. 16. Hourly accumulated water in comparison with the previous work vs. collector outlet temperatures.

temperature the performance of the two systems are relatively the same. Perhaps the remaining time of the flow inside the collector is the same.

6. Conclusions

A controlled flow solar water disinfecting system was experimentally installed and numerically validated as a solar thermal disinfection method to purify the biologically untreated water. It is found that the flat plate collector is capable to produce a considerable amount of disinfected water at different set temperatures corresponding to the water disinfecting levels. The annual accumulated water produced from the system is theoretically calculated. An accepted agreement between the simulated and measured accumulated clean water is obtained at different set point temperatures (60°C–90°C). It is found also that a good performance agreement between the present work and the previous edited work. A life-cycle savings analysis obtained that the flat-plate solar collector seems to be efficiently and economically used in solar water disinfecting systems. Based on the system outputs and economics, a large-scale of such systems can be considered in commercial use.

Symbols

A_c — Total collector array aperture area, m²
b_0 — Negative of the first-order coefficient of $(\tau\alpha)_b/(\tau\alpha)_n$ vs. $(1/\cos\theta - 1)$
b_1 — Negative of the second-order coefficient of $(\tau\alpha)_b/(\tau\alpha)_n$ vs. $(1/\cos\theta - 1)$
C — Commercial or non commercial flag (0 = non commercial, 1 = commercial)
C_A — Total area dependent costs, $/m².
C_c — Capacity rate of fluid on cold side, $\dot{m}_c C_{pc}$

C_E — Total cost of equipment which is independent of collector area, $
C_{FA} — Instantaneous auxiliary fuel cost rate, $/kJ
C_{FL} — Instantaneous conventional fuel cost rate, $/J
C_h — Capacity rate of fluid on hot side, $\dot{m}_h C_{ph}$
C_i — Coefficient of polynomial relating P/P_{max} to $\dot{m}/\dot{m}_{max}$
C_{max} — Maximum capacity rate
C_{min} — Minimum capacitance rate
C_p — Specific heat of fluid, J/kg.C
C_{pc} — Specific heat of collector fluid, J/kg.C
C_{ph} — Specific heat of hot side fluid of collector heat exchanger, J/kg.C
C_S — Total cost of all installed solar energy equipment, US$ = $C_A A + C_E$
d — Market discount rate
D — Ratio of down payments to total system investment
F' — Collector fin efficiency factor
f_{par} — Fraction of pump/fan power converted to fluid thermal energy
F_R — Overall collector heat removal efficiency factor
$F_R U_L$ — Negative of the first-order coefficient of collector efficiency vs. $F_R U_L/T$ and G_{test})
$F_R(\tau\alpha)$— Intercept of collector efficiency vs. $(T_i - T_a)/I_T$ for non normal incidence
$F_R(\tau\alpha)_n$— Intercept of collector efficiency vs. $(T_i - T_a)/I_T$ for normal incidence
G_{test} — Flow rate per collector unit area at test conditions, kg/m²
I — Total horizontal radiation per unit area, W/m²
I_{bT} — Incident beam radiation per unit area, W/m²
I_d — Horizontal diffuse radiation per unit area, W/m²
i_{FCF} — Conventional fuel inflation rate, %/y
ig — General inflation rate, %/y
IT — Total incident radiation on the collector surface, W/m²
LCS — Life cycle solar savings, US$
M — Accumulated water quantity, kg
m — Mortgage interest rate, %/y
m — Mass flow rate, kg/s
$\dot{m}_c$ — Collector fluid mass flow rate, kg/s
$\dot{m}_h$ — Fluid mass flow rate on hot side, kg/s
M_S — Extra insurance, maintenance, etc. in year one (% of original capital investment to the initial capital investment
N — Number of shell passes
N_D — Depreciation lifetime, y
N_E — Period of economic analysis, y
N_L — Period of loan, y
N'_{min} — Minimum of NE and ND, y
N_{min} — Years over which the mortgage payments contribute to the analysis
P — Power consumption of pump or fan, W
P_1 — Ratio of the life cycle fuel cost savings to the first year fuel cost savings
P_2 — Ratio of the life cycle expenditures incurred because of additional
P_{max} — Maximum power consumption (when $\gamma = 1$), W
PWF — Present worth factor
Q_{AUX} — Total auxiliary use for one year, J
Q_{load} — Total load for one year, J
$\dot{Q}_u$ — Rate of energy gain of total collector array, W
$\dot{Q}_T$ — Total heat transfer rate across heat exchanger, W
r_1 — Factor for correcting $F_R(\tau\alpha)_n$ and $F_R U'_L$ for operation at flow rates other than that at test conditions
SAL — Ratio of salvage value to initial investment
T — Temperature, °C
t — True property tax rate per dollar of original investment
$\bar{t}$ — Effective Federal State income tax rate
T_a — Ambiant temperature, °C
T_{ci} — Cold side inlet temperature, °C
T_{co} — Cold side outlet temperature, °C
T_{hi} — Hot side inlet temperature, °C
T_{ho} — Hot side outlet temperature, °C
T_g — Glass cover temperature, °C
T_i — Inlet fluid temperature, °C
T_o — Outlet fluid temperature, °C
T_{set} — Set temperature, °C
U_A — Overall heat transfer of heat exchanger, W/C
U_L — Overall loss coefficient of collector, W/m².C
V — Ratio of the assessed valuation of the solar energy system in the first year to the initial investment in the system

Greek

α — Absorptance of absorber plate
β — Collector slope (in degrees)
ε — Heat exchanger effectiveness
ε_1 — Heat exchanger effectiveness for one pass
γ — Control function ($0 \le \gamma \le 1$)
η — Collector efficiency
θ — Solar incidence angle(in degrees)
ρ_g — Ground reflectance of a flat-plate collector for ground reflected radiation
τ — Transmittance of the collector glass cover

Subscripts

b — Beam
g — Ground
i — Inlet
1–6 — Locations (Fig. 2)
n — Normal
o — Outlet
s — Diffuse

References

[1] D.A. Ciochetti and R.H. Metcalf, Pasteurization of naturally contaminated water with solar energy, Appl. Environ. Microbiol., 47(2) (1984) 223–228.

[2] N. Safapour and R. H. Metcalf, Enhancement of solar water pasteurization with reflectors, Appl. Environ. Microbiol., 65(2) (1999) 859–861.

[3] N.K. Bansal, R.L. Sawhney and A. Misra, Solar sterilization of water, Solar Energy, 1 (1988) 35–39.

[4] H.H. El-Ghetany and I.E. EL-Seesy, Performance evaluation of an overflow thermosyphon solar water heating system, Eng. Res. J., Helwan Univ., 101 (2005) M1–M16.

[5] I.E. El-Seesy, Solar water disinfecting system, Doctoral thesis, Department of Mechanical Engineering, Faculty of Engineering, Al-Azhar University, 2007.

[6] A.C. David and R.H. Metcalf, Pasteurization of naturally contaminated water with solar energy, Appl. Environ. Microbiol., (1984) 223–228.

[7] A.D. Shitzer, Z. Kalmanoviz and G. Grossman, Experiments with a flat plate solar water heating system in thermosyphonic flow, Solar Energy, 22 (1979) 27–35.

[8] G.L. Morrison and J.E. Braun, System modeling and operation characteristics of thermosyphon solar water heater, Solar Energy, 34 (1985) 389–405.

[9] M. Oates, P. Shanahan and M.F. Polz, Solar disinfection (SODIS): simulation of solar radiation for global assessment and application for point-of-use water treatment in Haiti, Wat. Res., 37 (2003) 47–54.

[10] O.A. McLoughlin, S.C. Kehoe, K.G. McGuigan, E.F. Duffy, A. Al Touati, Gernjak, I.O. Alberola, S.M. Rodríguez and L.W. Gill, Solar disinfection of contaminated water: a comparison of three small-scale reactors, Solar Energy, 77 (2004) 657–664.

[11] P. Fernández, J. Blanco, C. Sichel and S. Malato, Water disinfection by solar photocatalysis using compound parabolic collectors, Catalysis Today, 101 (2005) 345–352.

[12] A. Martin-Dominguez, M.T. Alarcoin-Herrera, I.R. Martin-Dominguez and A. Gonzailez-Herrera, Efficiency in the disinfection of water for human consumption in rural communities using solar radiation, Solar Energy, 78 (2005) 31–40.

[13] W.S. Duff and D.A. Hodgson, A simple high efficiency solar water purification system, Solar Energy, 79 (2005) 25–32.

[14] A. Scrivani, T. El Asmar and U. Bardi, Solar trough concentration for fresh water production and wastewater treatment, Desalination, 206 (2007) 485–493.

[15] A. Rinón and C. Pulgarin, Absence of *E. coli* regrowth after Fe^{3+} and TiO_2 solar photoassisted disinfection of water in CPC solar photoreactor, Catalysis Today, 124 (2007) 204–214.

[16] C. Navntoft, E. Ubomba-Jaswa, K.G. McGuigan and P. Fernández-Ibáñez, Effectiveness of solar disinfection using batch reactors with non-imaging aluminum reflectors under real conditions: Natural well-water and solar light, J. Photochem. Photobiol. B: Biol., 93 (2008) 155–161.

[17] J.A. Duffie and W.A. Beckman, Solar Engineering of Thermal Processes, J. Wiley & Sons, New York, 1991.

[18] ASHRAE Handbook of Fundamentals. American Society of Heating, Refrigeration, and Air Conditioning Engineers, Inc., Standard 93-77, 1977.

[19] F.P. DeWitt and D.P. Incropera, Introduction to Heat Transfer, J. Wiley and Sons, New York, 1996.

[20] M.J. Brandemuehl and W.A. Beckman, Economic evaluation and optimization of solar heating systems, Solar Energy, 23 (1979) 1–10.

[21] TRNSYS Coordinator, A Transient System Simulation Program, Madison: University of Wisconsin, 2000.